

Comment

Comment on Hamayun et al. Evaluation of Two-Column Air Separation Processes Based on Exergy Analysis. *Energies* 2020, 13, 6361

Miroslav Variny * , Dominika Jediná and Patrik Furda

Department of Chemical and Biochemical Engineering, Faculty of Chemical and Food Technology, Slovak University of Technology in Bratislava, Radlinského 9, 812 37 Bratislava, Slovakia; dominika.jedina@stuba.sk (D.J.); patrik.furda@stuba.sk (P.F.)

* Correspondence: miroslav.variny@stuba.sk

Abstract: Oxygen production from air belongs to energy-intensive processes and, as a result, possibilities for its decrease are a frequent topic of optimization studies, often performed with simulation software such as Aspen Plus or Aspen HYSYS. To obtain veritable results and sound solutions, a suitable calculation method hand in hand with justified assumptions and simplifications should form the base of any such studies. Thus, an analysis of the study by Hamayun et al., *Energies* 2020, 13, 6361, has been performed, and several weak spots of the study, including oversimplified assumptions, improper selection of a thermodynamic package for simulation and omission of certain technological aspects relevant for energy consumption optimization studies, were identified. For each of the weak spots, a recommendation based on good praxis and relevant scientific literature is provided, and general recommendations are formulated with the hope that this comment will aid all researchers utilizing Aspen Plus and Aspen HYSYS software in their work.



Citation: Variny, M.; Jediná, D.; Furda, P. Comment on Hamayun et al. Evaluation of Two-Column Air Separation Processes Based on Exergy Analysis. *Energies* 2020, 13, 6361. *Energies* 2021, 14, 6443. <https://doi.org/10.3390/en14206443>

Academic Editor: Noam Lior

Received: 18 June 2021

Accepted: 27 September 2021

Published: 9 October 2021

Publisher's Note: MDPI stays neutral with regard to jurisdictional claims in published maps and institutional affiliations.



Copyright: © 2021 by the authors. Licensee MDPI, Basel, Switzerland. This article is an open access article distributed under the terms and conditions of the Creative Commons Attribution (CC BY) license (<https://creativecommons.org/licenses/by/4.0/>).

Keywords: cryogenic air separation; oxygen production; Aspen Plus software; Peng–Robinson equation of state; process scheme; compressed air drying

1. Introduction

Oxygen is among the most frequently produced and consumed technical gases. It has found wide application in various industrial branches. Oxycombustion in the heat and power production sector [1,2] benefits from higher thermal efficiency of combustors [3] and subsequently reduced fuel consumption and lower carbon footprint [4,5], simultaneously offering the possibility for carbon capture and storage [6,7]. This is even more pronounced in the production and treatment of metals [8,9], where the achievable fuel and greenhouse gas reduction potential is substantial [10,11]. Oxygen use in gasification processes instead of air leads to products with increased heating value [12] and to reduced equipment size due to lower volumetric flows of the gaseous product [13]. As a result of the current COVID crisis, its importance as a medical gas has been fully revealed [14,15] and its production capacities are strained, which draws further attention to its impact on the environment [16,17].

Its production on an industrial scale is usually performed via cryogenic air separation [18,19]. Other techniques such as separation by membranes [20,21] or adsorption [22,23] have the potential to reduce the specific energy consumption for oxygen production but are still under development [24,25].

Cryogenic air separation is an energy-intensive process, which is the reason for the ongoing research effort for its design [26,27] and operation [28,29] optimization. It is, thus, of utmost importance that mathematical modeling of such units employs suitable thermodynamic models and adopts consistent and technically feasible assumptions. In this regard, we thoroughly analyzed the paper by Hamayun et al. (2020) [30] published previously

in the journal *Energies*. The performed analysis and the presented results are followed by generally valid recommendations for the modeling of cryogenic air separation units.

2. General Comments

Hamayun et al. (2020) [30] set up and analyzed seven different configurations of a cryogenic air separation plant with a processing capacity of 500 th⁻¹ of inlet air. They performed the underlying steady-state mathematical modeling in the Aspen Plus V10 environment using the Peng–Robinson property package. The Petlyuk-like column configuration came out as the most energy-effective one. In this section, general comments are formulated, while Section 3 provides more detailed comments on the plant scheme incorporating the Petlyuk-like column configuration, supported by our own simulations.

Firstly, model assumptions as formulated in [30] are incomplete. The pressure drop in heat exchangers assuming a constant value of 10 kPa, regardless of the position in the process scheme, is unjustified, similar to assuming zero pressure losses as in [26]. A more feasible approach is to adopt percentual pressure losses related to air inlet pressure. The Darcy–Weisbach equation, Equation (1), and the ideal gas state equation show that frictional pressure losses of gases and vapors depend on actual pressure (see Equation (2)), which justifies the proposed approach. This is also consistent with the approach of Szablowski et al. (2021) [31] where the assumed pressure drop in heat exchangers incorporated in the mathematical model of an adiabatic liquid energy storage system is related to the material stream density.

$$\Delta P = f \frac{L}{D} \rho \frac{v^2}{2} \quad (1)$$

$$\Delta P = f \frac{L}{D} \frac{pM}{RT} \frac{v^2}{2} \cong CP \quad (2)$$

where ΔP is the frictional pressure loss, Pa; f is a friction coefficient; L is the length and D is the inner diameter of the pipeline, both in m; ρ is the material stream density, kgm⁻³; v is the flow velocity, ms⁻¹; P is pressure of material stream, Pa; M is its molar mass, kgmol⁻¹; R is the universal gas constant; and T is the thermodynamic temperature of the material stream, in Kelvins. Assuming an adiabatic flow and small frictional pressure losses, then all variables in Equation (2) are almost constant and can, except for pressure, be merged into one constant, C .

Secondly, the authors omitted pressure losses in adsorbers. The issue of pressure loss in adsorbers is of serious concern and can be subject to optimization [32]. It contributes to the energy consumption of the air separation unit and should thus be considered.

Thirdly, adsorbers are modeled as component splitters, the assumption of which is oversimplified. The effect of water steam adsorption heat should be considered as it may reach up to 3000–4000 kJ·kg⁻¹ of adsorbed steam [33] for conventional zeolites used in compressed air drying by adsorption. The resulting temperature increase in air passing through the adsorbent layer can thus exceed 10 or even 20 °C depending on the water steam content in the inlet air which, in turn, impacts the equipment downstream.

Fourthly, the energy consumption evaluation in [30] is incomplete as it does not incorporate the energy needed for adsorber regeneration. As mentioned above, a significant amount of heat is released by steam adsorption on adsorbent, and thus, its regeneration is energy-intensive and contributes to the overall energy consumption of the air separation plant. Heat recuperation is often proposed to cut down the adsorbent regeneration costs [19,34], which, however, adds further complexity to the plant.

Fifthly, moist air cooling in a multi-stream heat exchanger directly to –100 °C and below after its intake from an ambient environment, as depicted in process scheme C7 in [30], is technically infeasible. It would lead to ice formation and air path blockage, possibly followed by heat exchanger damage.

The comments above document that proper and careful formulation of assumptions accompanied with a detailed check of each equipment piece modeled is a must before mathematical modeling. Moreover, the aspects discussed above affect the final energy

consumption of the air separation plant in individual configurations as the positions of the given equipment vary, as do their thermal duties and the mass flows of moisture removed from air.

Finally, the importance of using a proper thermodynamic package should be addressed. The Peng–Robinson equation is recommended for applications comprising non-polar gases and vapors [35], which holds true for nitrogen and oxygen or for dry air, but certainly not for water steam. We deal with this issue more deeply together with the chosen approach in Section 3.

3. Data Analysis Method

Following the model description and assumptions stated in [30], an identical model was set up in Aspen Plus® (Aspen Plus® V11, Aspen Technology Inc., Bedford, MA, USA) and Aspen HYSYS (Aspen HYSYS® V11, Aspen Technology Inc., Bedford, MA, USA). The scheme of the model set up in the Aspen Plus environment is shown in Figure 1.

Models in both Aspen Plus® and Aspen HYSYS served for verification of the model calculation results shown in [30]. Peng–Robinson as well as HYSR (Peng–Robinson for HYSYS) thermodynamic packages were tested for compression section modeling in Aspen Plus while Peng–Robinson was applied in Aspen HYSYS.

The Peng–Robinson equation of state is considered an ideal thermodynamic model to predict the phase equilibria during cryogenic air separation [36]. However, the model parameters and settings differ considerably between Aspen Plus and Aspen HYSYS.

The HYSR property method implements the Peng–Robinson property package from Aspen HYSYS into Aspen Plus. Several enhancements to the original Peng–Robinson model were made to extend its range of applicability and to improve its predictions for non-ideal systems [36].

First, Aspen Plus and Aspen HYSYS use different databanks for the estimation of bi-nary interaction parameters. Although most of the binary parameters are similar or the same, some of them, namely the parameters regarding the binary interactions of water, are different or missing.

Second, the way each model treats the missing parameters differs significantly. HYSR estimates the missing parameters from critical volume using Equation (3):

$$k_{ij} = \frac{1 - (V_{c,i}V_{c,j})^{1/6}}{0.5(V_{c,i}^{1/3} + V_{c,j}^{1/3})} \quad (3)$$

where k_{ij} is the binary interaction parameter, V_c is the critical volume and i and j are the respective components. However, no information is provided on how Aspen Plus treats the missing parameters, and according to the model results, it can be assumed that the Aspen Plus Peng–Robinson model considers no interaction where the information is missing. Furthermore, each model uses a different alpha function, although according to the values of acentric factors, this shall not make a difference when considering only the main air constituents.

Finally, and most importantly, specific attention needs to be given to the way both models treat water. Even though the user is asked about the steam tables to be used in the main settings pane, the default option of the Peng–Robinson model is not to use the steam tables. Hence, in order to attain comparable results, this option needs to be altered.

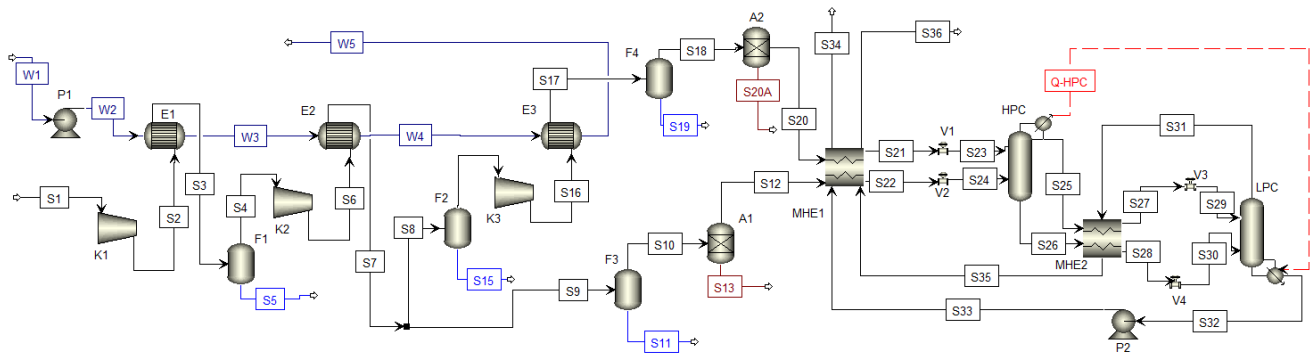


Figure 1. Mathematical model of air separation unit designed in Aspen Plus. Legend: A—adsorber; E—heat exchanger; F—phase separator; HPC—high-pressure column; K—compressor; LPC—low-pressure column; MHEX—multi-stream heat exchanger; P—pump; Q—energy stream; S—material stream except cooling water; V—valve; W—cooling water stream.

4. Results and Discussion

Simulation results for phase separators F1 to F4 are provided in Table 1. As can be seen, the results from Aspen Plus match those in [30] very closely. On the contrary, Aspen HYSYS yielded significantly lower mass flows of water condensate separated from air in the phase separators. To explain the different model outcomes, the Aspen Plus model was adjusted, switching from the standard Peng–Robinson package to the HYSPR package. The simulation results for phase separators F1 to F4 from Aspen Plus using the HYSPR package were compared with those from Aspen HYSYS as well as with data provided in [30] (Table 2). Switching from the Peng–Robinson to the HYSPR package in Aspen Plus resulted in data that are almost identical to those obtained from Aspen HYSYS. Thus, it can be stated that the differences in mass flows of water condensate from air visible in Table 1 resulted from the differences in the thermodynamic Peng–Robinson package implemented in Aspen Plus and in Aspen HYSYS.

Table 1. Simulation results for phase separators F1 to F4. Press. = pressure; Temp. = Temperature.

Stream	Aspen Plus			Aspen HYSYS			Study [30]		
	Mass Flow (kg/h)	Temp. (°C)	Press. (kPa)	Mass Flow (kg/h)	Temp. (°C)	Press. (kPa)	Mass Flow (kg/h)	Temp. (°C)	Press. (kPa)
S5 (F1)	0	40	240	0	40	240	0	40	240
S15 (F2)	459.3	40	590	244.4	40	590	500	40	590
S11 (F3)	976	40	590	519.3	40	590	1000	40	590
S19 (F4)	215.7	40	740	252.2	40	740	200	40	740

Table 2. Simulation results for phase separators F1 to F4 using the thermodynamic package HYSPR in Aspen Plus.

Stream	Aspen Plus			Aspen HYSYS			Study [30]		
	Mass Flow (kg/h)	Temp. (°C)	Press. (kPa)	Mass Flow (kg/h)	Temp. (°C)	Press. (kPa)	Mass Flow (kg/h)	Temp. (°C)	Press. (kPa)
S5 (F1)	0	40	240	0	40	240	0	40	240
S15 (F2)	244.4	40	590	244.4	40	590	500	40	590
S11 (F3)	519.2	40	590	519.3	40	590	1000	40	590
S19 (F4)	252.2	40	740	252.2	40	740	200	40	740

The mass flow of condensed water in exchanger E2 was further checked by hand calculation employing Equations (4)–(7). The mass flow of dry air was calculated first (Equation (4)), followed by calculation of the relative mass fraction of water vapor in air (Equation (5)). In the equations, m_G and m_{S7} are the mass flows of dry air and inlet air to heat exchanger E2, respectively, in kg h^{-1} ; w_{H_2O} is the mass fraction of water in

inlet air; and Y_{H_2O} is the relative mass fraction of water vapor in inlet air. $Y_{H_2O}^*$ is the equilibrium relative mass fraction of air leaving heat exchanger E2, which can be calculated by Equation (6), where $P_{H_2O}^\circ$ denotes the saturated vapor pressure of water, Pa; P is the overall pressure, Pa; and M_{H_2O} and M_G represent the molar masses of water and dry air, respectively, in kgmol^{-1} . The saturated vapor pressure of water at 40 °C, which is the air exit temperature from heat exchanger E2, was adopted from steam tables. The mass flow of water condensate from air in heat exchanger E2, \dot{m}_{H_2O} , kg h^{-1} , was calculated by Equation (7), and the results are shown in Table 3, where they are compared with the mass flows of condensed water obtained by Aspen Plus using the standard Peng–Robinson package and by Aspen HYSYS.

$$\dot{m}_G = \dot{m}_{S7} (1 - w_{H_2O}) = 500,000 \frac{\text{kg}}{\text{h}} \cdot (1 - 0.00976) = 495.12 \text{ kg/h} \quad (4)$$

$$Y_{H_2O} = \frac{w_{H_2O}}{1 - w_{H_2O}} = \frac{0.00976}{1 - 0.00976} = 0.0098561 \quad (5)$$

$$Y_{H_2O}^* = \frac{P_{H_2O}^\circ}{P - P_{H_2O}^\circ} \cdot \frac{M_{H_2O}}{M_G} = \frac{7.375 \text{ kPa}}{590 \text{ kPa} - 7.375 \text{ kPa}} \cdot \frac{18.02 \frac{\text{kg}}{\text{kmol}}}{28.96 \frac{\text{kg}}{\text{kmol}}} = 0.0078764 \quad (6)$$

$$\dot{m}_{H_2O} = \dot{m}_G \cdot (Y_{H_2O} - Y_{H_2O}^*) = 495,120 \frac{\text{kg}}{\text{h}} \cdot (0.0098561 - 0.0078764) = 980.2 \text{ kg/h} \quad (7)$$

Table 3. Simulation results: mass flows of water condensate in streams S7 and S19 obtained by simulations in Aspen Plus, Aspen HYSYS and by hand calculation (Equations (4)–(7)).

Stream	Aspen Plus	Aspen HYSYS	Hand Calculation
S7 (kg/h)	1435.3	763.7	980.4
S19 (kg/h)	215.7	252.2	254.7

As can be seen in Table 3, the hand calculation yielded values that are much closer to the results from Aspen HYSYS than to those from Aspen Plus using the standard Peng–Robinson package. This further corroborates the previous findings that the Peng–Robinson package implemented in Aspen HYSYS is more suitable for modeling processes involving water substance than the standard Peng–Robinson package in Aspen Plus.

Different predicted mass flows of water condensate separated in the phase separators further affect the water load of adsorbers A1 and A2. In reality, more water steam passes through the air compression and cooling train to the adsorbers than predicted in [30] using Aspen Plus. The difference in mass flows of water steam to be removed from compressed air in adsorbers A1 and A2 can be seen in Tables 4 and 5.

Table 4. Simulation results for adsorber A1.

A1									
Stream	Aspen Plus			Aspen HYSYS			Study [30]		
	Mass Flow (kg/h)	Temp. (°C)	Press. (kPa)	Mass Flow (kg/h)	Temp. (°C)	Press. (kPa)	Mass Flow (kg/h)	Temp. (°C)	Press. (kPa)
S10	339.0	40	590	339.5	40	590	339.0	40	590
S12	336.5	40	590	336.7	40	590	336.5	40	590
S13	2.5	40	590	2.8	40	590	2.5	40	590

Table 5. Simulation results for adsorber A2.

A1									
	Aspen Plus			Aspen HYSYS			Study [30]		
Stream	Mass Flow (kg/h)	Temp. (°C)	Press. (kPa)	Mass Flow (kg/h)	Temp. (°C)	Press. (kPa)	Mass Flow (kg/h)	Temp. (°C)	Press. (kPa)
S18	159.3	40	740	159.5	40	740	159.3	40	740
S20	158.4	40	740	158.4	40	740	158.4	40	740
S20A	0.9	40	740	1.1	40	740	1.0	40	740

The tables show that the mass flow of the remaining water steam to be removed is around 10% higher in Aspen HYSYS than in Aspen Plus using the standard Peng–Robinson thermodynamic package. This results in the need for a larger mass of adsorbent to be used in the adsorbers to maintain their operating time. Moreover, the adsorption heat release rate increases, and dry air leaves the adsorber at a higher temperature than that corresponding to the mass flows of adsorbed water predicted in [30]. It has to be stressed that the effect of adsorption heat is fully omitted in [30] as the adsorbers are treated as isothermal component splitters there. We consider such an approach to be oversimplified.

5. Recommendations for Future Work

From the detailed analysis of the cryogenic air separation unit simulation performed in [30], the following general recommendations can be drawn to increase the feasibility of the simulation results for similar or the same processes:

- Regarding pressure losses in gas or vapor heat exchangers, assuming a constant pressure loss value regardless of the actual thermodynamic conditions is an oversimplification. Adopting a percentual value related to the actual pressure of the given medium is recommended.
- Assuming isobaric–isothermal operation of water steam adsorbers from compressed air is infeasible. It is recommended to consider the adsorption heat effect properly and to consider air pressure loss in the adsorber at least equal to that in the preceding air cooler.
- Energy consumption for compressed air dryer (adsorber) regeneration should be taken into account, especially when performing an energy consumption optimization study.
- A proper thermodynamic package should be selected for modeling to avoid imprecise simulation results which may further affect the study findings and conclusions.

6. Conclusions

A thorough analysis of the study method and results presented in [30] was performed. Weak points of the method were discussed, such as the oversimplified assumptions, omitted thermal effects of water steam adsorption in adsorbers and the energy consumption for their regeneration as well as improper selection of the thermodynamic package, and recommendations for future work were formulated. It is hoped that the authors of [30] as well as other researchers find them helpful in their future research.

Author Contributions: Conceptualization, M.V.; methodology, D.J.; validation, P.F.; investigation, D.J. and M.V.; data curation, D.J.; writing—original draft preparation, M.V.; writing—review and editing, D.J. and P.F., visualization, D.J. All authors have read and agreed to the published version of the manuscript.

Funding: This study was supported by the Slovak Research and Development Agency under the contract no. APVV-18-0134.

Institutional Review Board Statement: Not applicable.

Informed Consent Statement: Not applicable.

Data Availability Statement: All data obtained by calculations and analyses are listed directly in this study.

Conflicts of Interest: The authors declare no conflict of interest. The funders had no role in the design of the study; in the collection, analyses, or interpretation of data; in the writing of the manuscript, or in the decision to publish the results.

References

1. Ghoniem, A.F.; Zhao, Z.; Dimitrakopoulos, G. Gas oxy combustion and conversion technologies for low carbon energy: Fundamentals, modeling and reactors. *Proc. Combust. Inst.* **2019**, *37*, 33–56. [[CrossRef](#)]
2. Kotowicz, J.; Michalski, S.; Brzeczek, M. The Characteristics of a Modern Oxy-Fuel Power Plant. *Energies* **2019**, *12*, 3374. [[CrossRef](#)]
3. Portillo, E.; Gallego Fernández, L.M.; Vega, F.; Alonso-Fariñas, B.; Navarrete, B. Oxygen transport membrane unit applied to oxy-combustion coal power plants: A thermodynamic assessment. *J. Environ. Chem. Eng.* **2021**, *9*, 105266. [[CrossRef](#)]
4. Normann, F.; Andersson, K.; Johnsson, F.; Leckner, B. NOx reburning in oxy-fuel combustion: A comparison between solid and gaseous fuels. *Int. J. Greenh. Gas. Control* **2011**, *5*, S120–S126. [[CrossRef](#)]
5. Bělohradský, P.; Skryja, P.; Hudák, I. Experimental study on the influence of oxygen content in the combustion air on the combustion characteristics. *Energy* **2014**, *75*, 116–126. [[CrossRef](#)]
6. Fogarasi, S.; Cormos, C.-C. Assessment of coal and sawdust co-firing power generation under oxy-combustion conditions with carbon capture and storage. *J. Clean. Prod.* **2017**, *142*, 3527–3535. [[CrossRef](#)]
7. Allam, R.; Martin, S.; Forrest, B.; Fetvedt, J.; Lu, X.; Freed, D.; Brown, G.W.; Sasaki, T.; Itoh, M.; Manning, J. Demonstration of the Allam Cycle: An Update on the Development Status of a High Efficiency Supercritical Carbon Dioxide Power Process Employing Full Carbon Capture. *Energy Procedia* **2017**, *114*, 5948–5966. [[CrossRef](#)]
8. Royo, P.; Ferreira, V.J.; López-Sabirón, A.M.; García-Armingol, T.; Ferreira, G. Retrofitting strategies for improving the energy and environmental efficiency in industrial furnaces: A case study in the aluminium sector. *Renew. Sustain. Energy Rev.* **2018**, *82*, 1813–1822. [[CrossRef](#)]
9. Dzurňák, R.; Varga, A.; Kizek, J.; Jablonský, G.; Lukáč, L. Influence of Burner Nozzle Parameters Analysis on the Aluminium Melting Process. *Appl. Sci.* **2019**, *9*, 1614. [[CrossRef](#)]
10. Poskart, A.; Radomiak, H.; Niegodajew, P.; Zajemska, M.; Musiał, D. The Analysis of Nitrogen Oxides Formation During Oxygen—Enriched Combustion of Natural Gas. *Arch. Metall. Mater.* **2016**, *61*, 1925–1930. [[CrossRef](#)]
11. Dzurňák, R.; Jablonský, G.; Varga, A.; Kizek, J.; Pástor, M.; Lukáč, L. Impact of oxygen enhanced combustion of natural gas on thermal efficiency of combustion aggregate. *MATEC Web Conf.* **2018**, *168*, 07016. [[CrossRef](#)]
12. Gabbar, H.; Aboughaly, M.; Russo, S. Conceptual Design and Energy Analysis of Integrated Combined Cycle Gasification System. *Sustainability* **2017**, *9*, 1474. [[CrossRef](#)]
13. Corti, A. Biomass integrated gasification combined cycle with reduced CO₂ emissions: Performance analysis and life cycle assessment (LCA). *Energy* **2004**, *29*, 2109–2124. [[CrossRef](#)]
14. Carnero, M.C.; Gómez, A. Optimization of Decision Making in the Supply of Medicinal Gases Used in Health Care. *Sustainability* **2019**, *11*, 2952. [[CrossRef](#)]
15. Feinmann, J. How covid-19 revealed the scandal of medical oxygen supplies worldwide. *BMJ* **2021**, *373*, n1166. [[CrossRef](#)]
16. Balys, M.; Brodawka, E.; Korzeniewska, A.; Szczurowski, J.; Zarebska, K. LCA and economic study on the local oxygen supply in Central Europe during the COVID-19 pandemic. *Sci. Total. Environ.* **2021**, *786*, 147401. [[CrossRef](#)]
17. Shakil, M.H.; Munim, Z.H.; Tasnia, M.; Sarowar, S. COVID-19 and the environment: A critical review and research agenda. *Sci. Total. Environ.* **2020**, *745*, 141022. [[CrossRef](#)]
18. Xu, J.; Wang, T.; Chen, Q.; Zhang, S.; Tan, J. Performance design of a cryogenic air separation unit for variable working conditions using the lumped parameter model. *Front. Mech. Eng.* **2019**, *15*, 24–42. [[CrossRef](#)]
19. Wang, C.; Akkurt, N.; Zhang, X.; Luo, Y.; She, X. Techno-economic analyses of multi-functional liquid air energy storage for power generation, oxygen production and heating. *Appl. Energy* **2020**, *275*, 115392. [[CrossRef](#)]
20. Adhikari, B.; Orme, C.J.; Klaehn, J.R.; Stewart, F.F. Technoeconomic analysis of oxygen-nitrogen separation for oxygen enrichment using membranes. *Sep. Purif. Technol.* **2021**, *268*, 118703. [[CrossRef](#)]
21. Dibrov, G.; Ivanov, M.; Semyashkin, M.; Sudin, V.; Fateev, N.; Kagramanov, G. Elaboration of High Permeable Macrovoid Free Polysulfone Hollow Fiber Membranes for Air Separation. *Fibers* **2019**, *7*, 43. [[CrossRef](#)]
22. Banaszkiwicz, T.; Chorowski, M. Energy Consumption of Air-Separation Adsorption Methods. *Entropy* **2018**, *20*, 232. [[CrossRef](#)] [[PubMed](#)]
23. Akulinin, E.; Golubyatnikov, O.; Dvoretzky, D.; Dvoretzky, S. Optimization and analysis of pressure swing adsorption process for oxygen production from air under uncertainty. *Chem. Ind. Chem. Eng. Q.* **2020**, *26*, 89–104. [[CrossRef](#)]
24. Fernandez-Barquin, A.; Casado-Coterillo, C.; Valencia, S.; Irabien, A. Mixed Matrix Membranes for O₂(2)/N₂(2) Separation: The Influence of Temperature. *Membranes* **2016**, *6*, 28. [[CrossRef](#)] [[PubMed](#)]
25. Widiastuti, N.; Gunawan, T.; Fansuri, H.; Salleh, W.N.W.; Ismail, A.F.; Szali, N. P84/ZCC Hollow Fiber Mixed Matrix Membrane with PDMS Coating to Enhance Air Separation Performance. *Membranes* **2020**, *10*, 267. [[CrossRef](#)] [[PubMed](#)]
26. Caspari, A.; Offermanns, C.; Schäfer, P.; Mhamdi, A.; Mitsos, A. A flexible air separation process: 1. Design and steady-state optimizations. *AIChE J.* **2019**, *65*, e16705. [[CrossRef](#)]

27. Singla, R.; Chowdhury, K. Enhanced oxygen recovery and energy efficiency in a reconfigured single column air separation unit producing pure and impure oxygen simultaneously. *Chem. Eng. Process. Process Intensif.* **2021**, *162*, 108354. [[CrossRef](#)]
28. Adamson, R.; Hobbs, M.; Silcock, A.; Willis, M.J. Steady-state optimisation of a multiple cryogenic air separation unit and compressor plant. *Appl. Energy* **2017**, *189*, 221–232. [[CrossRef](#)]
29. Elhelw, M.; Alsanousie, A.A.; Attia, A. Novel operation control strategy for conjugate high-low pressure air separation columns at different part loads. *Alex. Eng. J.* **2020**, *59*, 613–633. [[CrossRef](#)]
30. Hamayun, M.H.; Ramzan, N.; Hussain, M.; Faheem, M. Evaluation of Two-Column Air Separation Processes Based on Exergy Analysis. *Energies* **2020**, *13*, 6361. [[CrossRef](#)]
31. Szablowski, L.; Krawczyk, P.; Wolowicz, M. Exergy Analysis of Adiabatic Liquid Air Energy Storage (A-LAES) System Based on Linde–Hampson Cycle. *Energies* **2021**, *14*, 945. [[CrossRef](#)]
32. Shigaki, N.; Mogi, Y.; Haraoka, T.; Sumi, I. Reduction of Electric Power Consumption in CO₂-PSA with Zeolite 13X Adsorbent. *Energies* **2018**, *11*, 900. [[CrossRef](#)]
33. Kim, H.; Cho, H.J.; Narayanan, S.; Yang, S.; Furukawa, H.; Schiffres, S.; Li, X.; Zhang, Y.B.; Jiang, J.; Yaghi, O.M.; et al. Characterization of Adsorption Enthalpy of Novel Water-Stable Zeolites and Metal-Organic Frameworks. *Sci. Rep.* **2016**, *6*, 19097. [[CrossRef](#)] [[PubMed](#)]
34. Goodarzia, G.; Dehghani, S.; Akbarzadeh, A.; Date, A. Energy Saving Opportunities in air Drying Process in High-pressure Compressors. *Energy Procedia* **2017**, *110*, 428–433. [[CrossRef](#)]
35. Haydary, J. *Chemical Engineering Process. Design and Simulation-Aspen Plus and Aspen HYSYS Applications*, 1st ed.; Wiley & Sons, Inc.: Hoboken, NJ, USA, 2019.
36. Aspen Technology Inc. *Aspen Plus User Guide, Version 10.2*; Aspen Technology Inc.: Cambridge, MA, USA, 2000.